Received: 21 December 2022 | Accepted: 21 December 2022

DOI: 10.1111/ahe.12900

Anatomia Histologia Embryologia | WILEY

ORIGINAL ARTICLE

Anatomical and pathological characteristics of ribs in the Atlantic salmon (*Salmo salar* L.) and its relevance to soft tissue changes

Malin Brimsholm[1] | Per Gunnar Fjelldal[2] | Tom Hansen[2] | Cathrine Trangerud[3] | Geir Magne Knutsen[4] | Charlotte Finstad Asserson[4] | Erling Olaf Koppang[1] | Håvard Bjørgen[1]

[1]Unit of Anatomy, Faculty of Veterinary Medicine, Norwegian University of Life Sciences, Ås, Norway

[2]Matre Research Station, Institute of Marine Research, Matredal, Norway

[3]Unit of Radiology, Faculty of Veterinary Medicine, Norwegian University of Life Sciences, Ås, Norway

[4]Bremnes Seashore, Bremnes, Norway

Correspondence
Håvard Bjørgen, Unit of Anatomy, Faculty of Veterinary Medicine, Norwegian University of Life Sciences, 1433 Ås, Norway.
Email: havard.bjorgen@nmbu.no

Funding information
Fiskeri - og havbruksnæringens forskningsfond, Grant/Award Number: 901501

Abstract

Studies on the anatomical and pathological characteristics of ribs in farmed Atlantic salmon (*Salmo salar* L.) are warranted due to their possible association with red and melanized focal changes (RFC and MFC) in the fillet, a major quality and animal welfare concern. In this work, we provide an anatomical description of ribs based on radiographical and histological analyses. We also address various pathological rib changes and their association to RFC and MFC. In total, 129 fish were investigated; captured wild ($n = 10$) and hatchery reared ($n = 119$) Atlantic salmon (3.5–6.1 kg). The fish were selected based on the macroscopic presence of RFC, MFC or no changes (controls). Radiographic results revealed costal abnormalities in all fish groups. By histological investigations of the variations herein, our results provide new insight into the anatomical characteristics including vascularization within the ribs; a potential site for haemorrhage following costal fractures. Costal fractures were detected by radiology in 40 of 129 samples (RFC: 38.4%, MFC: 47.2%, controls: 9.5 %). A statistically significant association was found between costal fractures and red ($p = 0.007$) and melanized changes ($p = 0.000$). However, red and melanized changes were also observed in samples with no costal fractures ($n = 45$), indicating that also other factors influence the development of RFC/MFC.

KEYWORDS
Atlantic salmon, fillet, histology, melanin, radiology, ribs

1 | INTRODUCTION

Teleost bones show many similar morphological traits to mammalian bones. Both mammalian and teleost bone collars are covered by periosteum, and cortical bone is oriented in longitudinal lamellas surrounding a medullar cavity lined with endosteum (Cohen et al., 2012; Davesne et al., 2019; Jiao et al., 2020; Moss, 1961, 1962; Weiss & Watabe, 1979; Witten & Huysseune, 2009). Salmonids are regarded as primitive teleosts (Davesne et al., 2019), in which a characteristic trait is the presence of osteocytes embedded in the lamellar bone classified as cellular bone, as found in mammals (Moss, 1961;Moss, 1963). Advanced teleost species such as tilapia

(*Oreochromis niloticus*) and medaka (*Oryzias latipes*) are classified with acellular bone, that is, bone lacking embedded osteocytes (Boglione et al., 2013; Cohen et al., 2012; Kölliker, 1857; Moss, 1961). Bone formation is performed through perichondral, endochondral or intramembranous ossification and in large teleosts such as the Atlantic salmon (*Salmo salar*), the presence of spongious bone has been described (Moss, 1961, 1963; Weigele & Franz-Odendaal, 2016; Witten et al., 2000; Witten & Hall, 2002). In contrast to mammals, teleosts have no functional bone marrow in the medullar cavity of the bone (reviewed by Bjørgen & Koppang, 2021). The medullar cavity consists of either chondrocytes or, after resorption of cartilage by chondroclasts, adipose tissue (Boglione et al., 2013; Jiao et al., 2020; Moss, 1963; Weigele & Franz-Odendaal, 2016; Willett et al., 1999; Witten et al., 2001; Witten & Huysseune, 2009).

In teleost fish, the ribs (*costae*) are part of the axial skeleton, extending from the vertebral bodies in a ventrolateral direction into the sub-peritoneal fascia on both sides of the abdominal cavity (Kryvi & Poppe, 2016; Roberts, 2012). Investigations done on silver carp (*Hypophthalmichthys molitrix*) have shown that the ribs develop by perichondral ossification with an elongation process through type II endochondral ossification, with no bone tissue formed in the medullar cavity (Soliman, 2018). Together with the thick abdominal musculature and covered by parietal peritoneum, the ribs function as a protective shield for the abdominal organs. They also act as anchors for muscle attachment, thus contributing to the swimming movement of the fish. Although the structure of ribs in fish, including Atlantic salmon, has been described in previous reports (Horton & Summers, 2009; Jiao et al., 2020; Jiménez-Guerrero et al., 2022; Kague et al., 2019; Nie et al., 2017; Patterson & Johnson, 1995; Roberts, 2012; Soliman, 2018), studies on the anatomy of ribs in farmed Atlantic salmon with a broad histological approach are scarce. In farmed salmon and other reared fish species, pathological changes and deformities in bones are not uncommon and have been associated with several production-related factors (Aunsmo et al., 2008; Baeverfjord et al., 1998; Boglione et al., 2014; Eriksen et al., 2006; Gil Martens et al., 2010; Gislason et al., 2010; Martini et al., 2021). Insufficient diet giving phosphorus, ascorbic acid and vitamin D deficiency has been proved to affect bone development and bone weakness in both mammals and teleosts (Baeverfjord et al., 1998; Darias et al., 2011; Roberts et al., 2001). In salmonids, vertebral deformities have been reported as the most frequent skeletal abnormality, with several different malformations in the vertebral column such as lordosis, kyphosis and scoliosis, vertebral fusions and cross-stich vertebra (Fjelldal et al., 2012; Trangerud et al., 2020; Witten et al., 2009). Thus, most studies have focused on changes in the vertebra, and not the ribs.

Costal changes seem especially interesting in relation to the condition termed melanized focal changes (MFC), which is a major quality concern in the fillet of farmed salmon. Such changes are typically restricted to a focal area in the cranio-ventral part of the fillet (Bjørgen et al., 2019), with affected musculature reaching medially from underneath the peritoneum and continuing towards the red musculature laterally. Based on primarily radiological analysis, an association between costal abnormalities and MFC was reported by Jiménez-Guerrero et al. (2022). However, MFC were also found in fish without costal abnormalities, and environmental factors were suggested to be determinant for the development of MFC (Jiménez-Guerrero et al., 2022). The average prevalence of MFC at slaughter is about 20% (Mørkøre et al., 2015), and their occurrence is a reason for downgrading or cassation, leading to substantial economic losses. In the early stage of the condition, a focal haemorrhage occurs in the same restricted area. These changes appear red (macroscopically) and have thus been termed red focal changes (RFC). Histologically, acute necrosis and extra-vasal erythrocytes dominate within the tissue (Bjørgen et al., 2019, 2020). As the RFC develop, the tissue becomes increasingly necrotic and fibrotic, and leukocytes are recruited to the area. Among these are the melano-macrophages, a pigment-producing leukocyte responsible for the discolouration of the fillet. Instead of healing, a chronic granulomatous inflammatory condition may develop, sometimes with well-organized granulomas (Koppang et al., 2005; Larsen et al., 2012). This state of the condition has been associated with the presence of piscine orthoreovirus 1 (PRV-1) (Bjørgen et al., 2015, 2019). PRV-1 antigen has been shown to be walled off in granulomas, and local replication of PRV-1 is believed to be the driving power of this non-resolving condition (Bjørgen et al., 2020). However, RFC can occur prior to PRV-1 infection (Bjørgen et al., 2019), and their initial cause is still unknown. Their restricted focal location argues for an underlying anatomical predisposition, possibly associated with costal injury and/or costal fractures. In mammals, but also in fish, bone fractures can affect the neighbouring soft tissue and can cause haemorrhage (de Haan et al., 2016). This in turn is followed by acute inflammation (Loi et al., 2016; Marsell & Einhorn, 2011; Schindeler et al., 2008). Thus, a similar pathogenesis is possible in salmon, where haemorrhage and acute inflammation following a costal fracture may develop into a chronic, granulomatous inflammation driven by the presence of PRV-1.

The overall aim of this study was to investigate variations in costal anatomy in Atlantic salmon, herein addressing various changes in the ribs and in the neighbouring musculature, possibly leading to the development of RFC/MFC. This was approached by collecting a comprehensive material from different groups of fish including farmed, wild, and experimentally kept fish, where samples of both affected (RFC/MFC) and unaffected musculature were collected. By performing macroscopic, radiographic and histological investigations, we describe the anatomical features, the different pathological changes and the association between such changes and RFC/MFC.

2 | MATERIALS AND METHODS

2.1 | Fish origin

Fillets containing ribs were obtained from three different locations in Norway (Table 1). In total, we studied the ribs and adjacent soft tissue in relation to RFC and MFC from 129 individuals.

TABLE 1 Fish origin and key information

Population	Location	Samples (*n*)	Sea transfer (date)	Harvest (week)	Weight at slaughter (mean)	Vaccination	Diagnosis
1	Bremnes Seashore	40	21.11.2017	21/2019	4.70 kg	Aquavet PD 7 VET	PD, CMS
2	Bremnes Seashore	18	17.03.2018	26/2019	3.50 kg	Alpha Ject Micro 1 PD/6	PD, CMS, HSMI
3	Bremnes Seashore	32	08.09.2019	5/2021	5.99 kg	Alpha Ject Micro 1 PD/6	PD, CMS patraurellosis
4	Bremnes Seashore	6	21.09.2021	34/2022	4.10kg	Aquavaq 6	Pastaurellosis, mycobacteriosis, PRV[a], PMCV[a]
5	Matre Research St.	23	22.05.2018 20.08.2018	36/2019	4.39 kg	Aquavac 6	PRV[a]
6	Drammenselven	6 4	x x	46/2019 48/2020	6.13 kg 5.1kg	x x	PRV[a]

[a]Virus detected by RT-qPCR, but diagnosis not confirmed.

A total of six different samplings were conducted (population 1–6; Table 1), where population 1–4 were collected at slaughter, originating from a commercial aquaculture facility, Bremnes Seashore, Bømlo, Norway. Population 5 included farmed, wild and farmed X wild hybrid salmon from Matre Research Station, Institute of Marine Research, Matre, Norway. The farmed salmon in this population were of MOWI origin, and the wild salmon were obtained from wild caught parent's eggs and sperm fertilized at the premises in Matre. Hybrids represented a combination of wild and farmed eggs and sperm. After hatching, wild, farmed and hybrid fish were kept under common rearing conditions, i.e., tanks and sea water cages (Debes et al., 2021). Population 6 consisted of wild spawning salmon caught in the river Drammenselven in the eastern part of Norway.

2.2 | Sample handling and macroscopic evaluation

At slaughter, the fillets were sampled based on macroscopic evaluation of the abdominal wall, that is, peritoneum, ribs and adjacent white skeletal muscle. Fillets with no appearent discolouration were sampled as controls. Macroscopic discolouration included RFC and MFC and was graded using the classification system developed by MOWI, with grades from 0 to 3 with increasing severity (Bjørgen et al., 2019). The sampling of population 1–4 was conducted by the staff at Bremnes Seashore and shipped on ice to the Norwegian School of Veterinary Science (NMBU), Adamstuen, Oslo. Here, the samples were transferred to buffered formalin for fixation. The samples in population 5 and 6 were also collected at the time of slaughter/spawning and were transferred to formalin immediately after dissection. The weight and length of each fish in these populations were registered prior to dissection. Samples from population 1–4 and 6 included the ribs in their total length, while in population 5, samples were retrieved only from the area with macroscopic discolouration and equivalent areas for controls.

Prior to radiographic investigations, the abdominal walls were palpated to reveal costal abnormalities and fractures. The size of the samples in population 1–4 and 6 were approximately 10 × 15 cm, as for population 5 the sample size was about 5 × 6 cm, with some variation. Prior to fixation in buffered formalin, all samples but for population 5 were photographed to record macroscopic information. For further investigations, the samples were grouped according to discolouration and arranged into groups; group A: No macroscopic discolouration; group B: RFC and group C: MFC.

2.3 | Radiographic investigations

Radiographic investigations were conducted at the radiology department at the NMBU premises on Adamstuen, by a direct digital system (SoundEklineSeries DR). The samples were labelled according to population and sample number and then placed on trays in order of correct numbering. The samples from Bremnes were

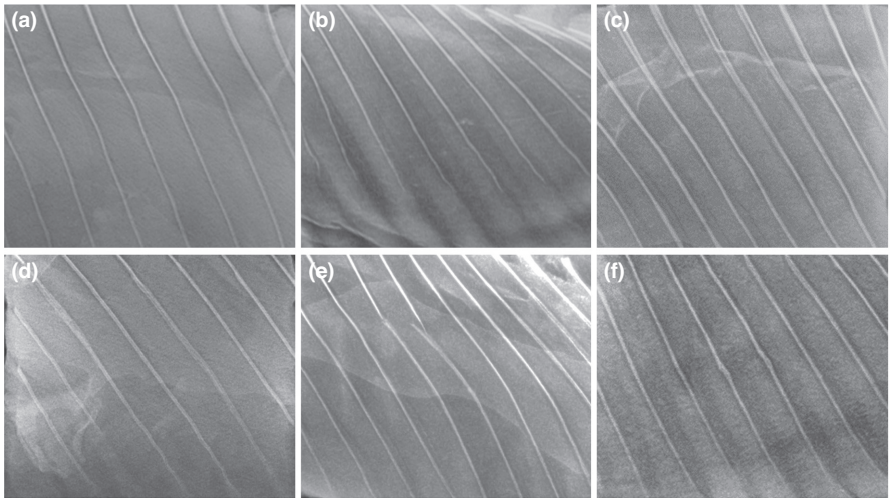

FIGURE 1 Radiological results, ribs in farmed Altantic salmon (*Salmo salar L.*) lateral aspect. (a) Proximal part of ribs showing axis deviation noted as mild bending of axis. (b) Distal part of ribs showing axis deviations noted as wave shaped ribs. (c) Proximal part of ribs with a central radiolucent medulla. (d) Mid part of ribs with focal radiolucent appearance. Distal parts of ribs are also wave shaped. (e) Mid part of rib with costal fracture. (f) Distal part of ribs with focal thickening noted as callus formations.

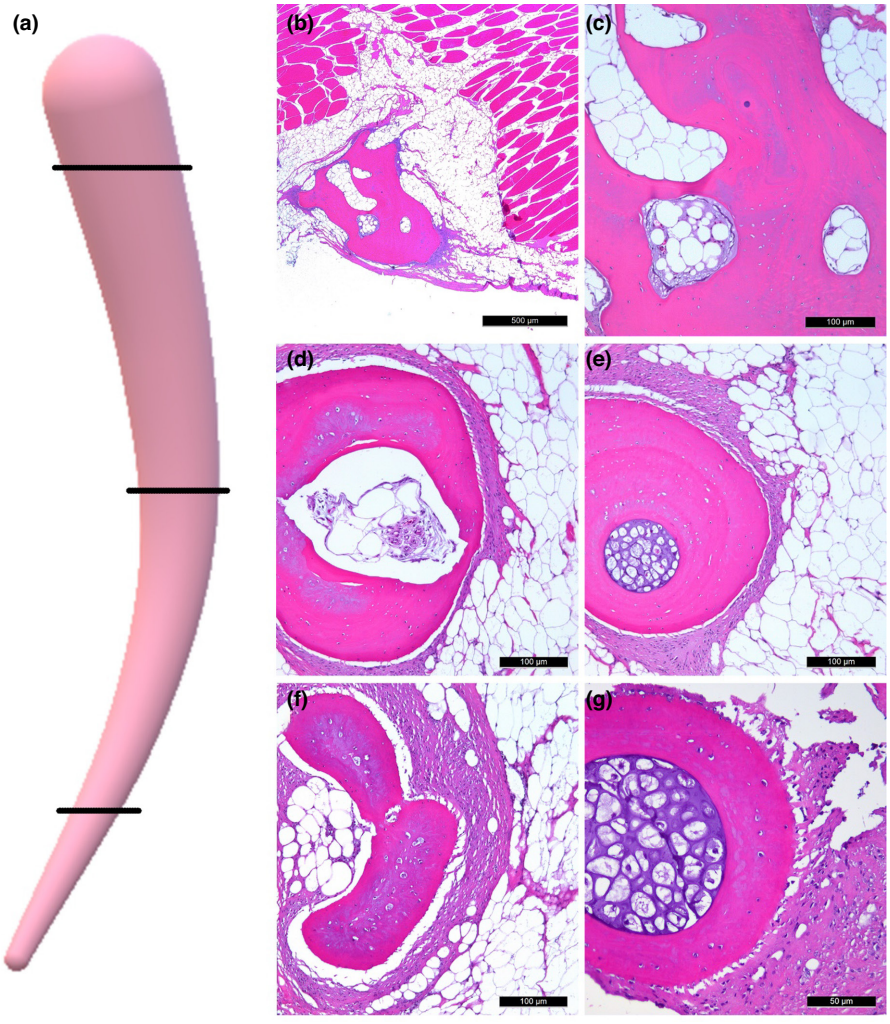

FIGURE 2 Atlantic salmon ribs. Schematic illustration of ribs (a), with cross sections showing variations of proximal (b, c), mid (d, e) and distal (f, g) parts. All sections are retrieved from the same individual (farmed salmon). Note the different scale bars in proximal and distal parts. (b) Proximal part, irregular circumference of rib with several large cavities in the cortical bone. Scale bar: 500 µm. (c) Proximal part, higher magnification of section seen in 'b'. Cavities in the cortical bone containing adipocytes. Blood vessels in the medullar cavity. Scale bar: 100 µm. (d) Mid part, round circumference. Medullar cavity with blood vessels. Scale bar: 100 µm. (e) Mid part, round circumference. Medullar cavity containing chondrocytes. Scale bar: 100 µm. (f) Distal part, irregular circumference. No apparent medullar cavity seen. Scale bar: 100 µm. (g) Distal part, round circumference. Medullar cavity containing chondrocytes. Scale bar: 50 µm.

radiographed in groups of 6, while the samples from Matre were radiographed in groups of 12, as the samples were smaller. The first six samples in population 6 were not radiologically examined, and the last four samples were radiographed in one group. After radiography, the samples were returned to buffered formalin to avoid dehydration.

2.4 | Statistical analyzes

To investigate association between costal changes and macroscopic discolouration, a chi-squared test followed by a logistic regression was conducted using STATA (StataCorp. 2019. Stata Statistical Software: Release 16: StataCorp LLC).

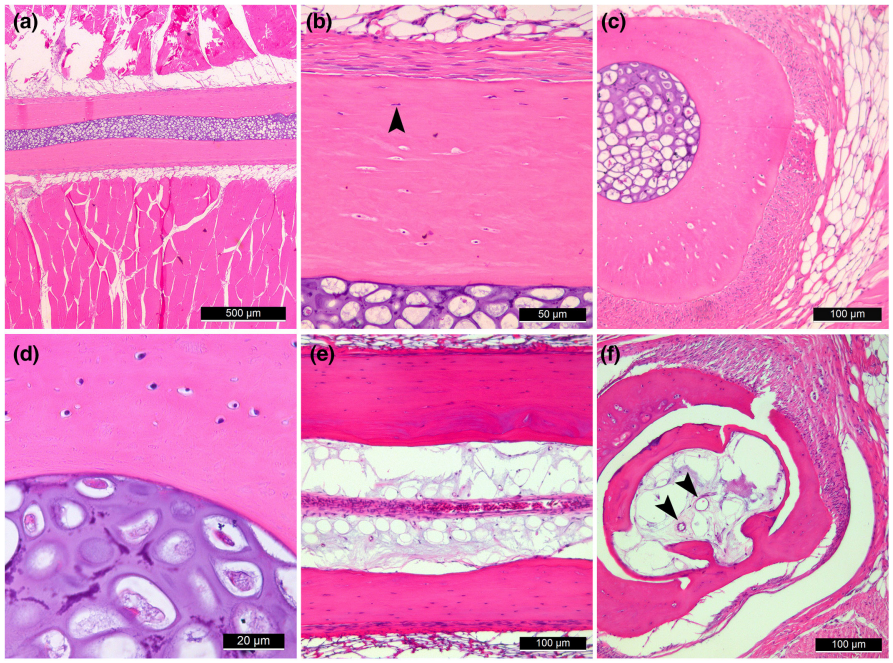

FIGURE 3 Histological investigation, group A. Anatomical characteristics of ribs and adjacent soft tissue in farmed and wild Atlantic salmon with no detected costal or adjacent soft tissue changes. All sections are retrieved from wild salmon. (a) Longitudinal section of rib. Hypertrophic chondrocytes in the medullar cavity and adjacent soft tissue, that is, adipose tissue and white skeletal muscle. Scale bar: 500 µm. (b) Longitudinal section. Osteocytes (arrowhead) embedded in the cortical bone, with parallel-oriented lamellae. Periosteum covering the bone collar. Scale bar: 50 µm. (c) Cross section. Chondrocyttic core, cortical bone and adjacent soft tissue surrounding the rib. Scale bar: 100 µm. (d) Cross section. Osteocytes embedded in bone tissue, no apparent osteons. (e) Longitudinal section. Medullar cavity with adipose tissue and a longitudinal oriented blood vessel. Scale bar: 100 µm. (f) Cross section. Medullar cavity with adipose tissue and multiple vessels seen (arrowhead). Scale bar: 100 µm.

2.5 | Histological investigations

Following fixation and radiological investigations, the samples were decalcified in 0.5 M pH 8 EDTA solution (disodium ethylenediaminetetraacetate, 2H2O) for a minimum of five days, according to size. The samples were further sectioned for block preparation to include the area containing RFC or MFC, and/or costal abnormalities revealed by radiographic investigations. Following paraffin embedding performed according to standard procedures, the slides were sectioned in 2 µm thickness and transferred to glass slides. After incubation at 37°C for 36–48 h, the sections were deparaffinized in xylene, rehydrated through alcohol baths and stained according to standard haematoxylin and eosin staining protocols.

2.6 | Pathogen detection

Farmed salmon in population 1–4 originated from larger fish groups at Bremnes Seashore, Bømlo. Registered diagnoses were detected through fish health and pathogen surveillance at the production site (Table 1). In population 5 and 6, samples from spleen were collected on RNA*later* and sent to PatoGen AS, Ålesund, Norway, for RT-qPCR-analysis accredited and validated to ISO7025 standards for the detection of piscine orthoreovirus 1 (PRV-1).

3 | RESULTS

3.1 | Macroscopic evaluation and classification of changes

Macroscopic evaluation was conducted in each population (1–6). In population 1 (Bremnes), six samples contained RFC, 29 samples contained MFC and five samples had no macroscopic discolouration. In population 2 (Bremnes), seven samples contained RFC and 11 samples contained MFC. In population 3 (Bremnes), 12 samples contained RFC, one sample contained MFC and the remaining 19 samples had no macroscopic discolouration. None of the samples in population 4 (Bremnes) showed macroscopic discolouration. In population 5 (Matre), one sample had RFC, 14 samples had MFC, and eight samples showed no macroscopic discolouration. No macroscopic discolouration was detected in population 6 (wild salmon). Changes in population 1, 2 and 3 were located mainly in the ventral area of the abdominal wall. All changes were graded 1–3. Based on macroscopic evaluation, the samples were grouped accordingly: No macroscopic discolouration (group A) $n = 48$, RFC (group B) $n = 26$, MFC (group C) $n = 55$.

In group B, seven samples were classified as grade 3, while the rest showed mild discolouration; nine samples with grade 2 and ten samples with grade 1. Mixed changes (red and melanized combined) were present in three samples, but haemorrhage dominated

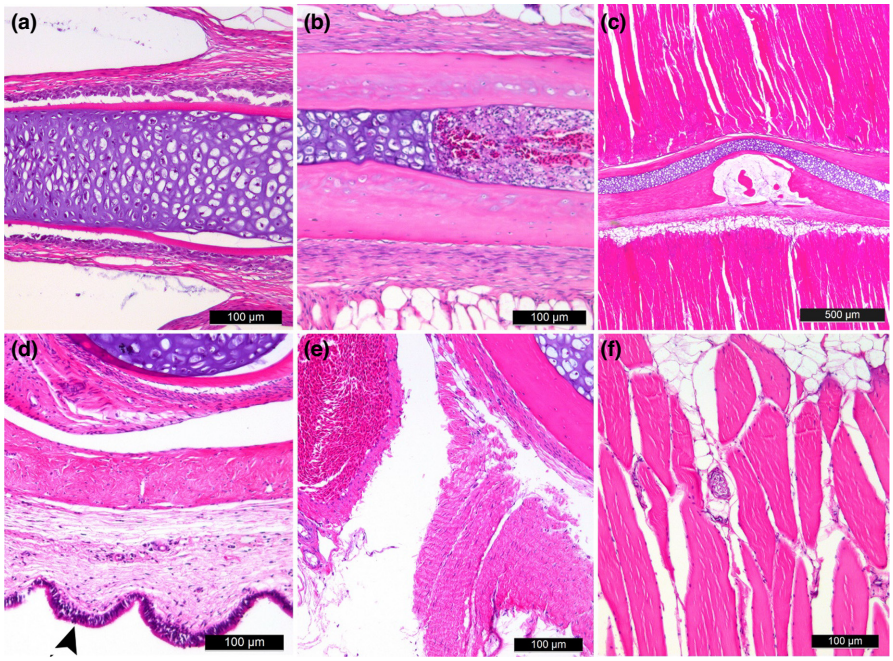

FIGURE 4 Histological investigation, group A. Anatomical characteristics of ribs and adjacent soft tissue in farmed and wild Atlantic salmon with no detected costal or adjacent soft tissue changes. (a) Farmed salmon. Distal part of rib containing a zone of proliferative chondrocytes in the medullar cavity. Hyperthrophic chondrocytes seen on the right. Scale bar: 100 µm. (b) Farmed salmon. Rib showing central medulla with abrubt demarcation in the transitional zone. The chondrocytic core is intact prior to the transitional zone. Blood vessels and cell infiltration post transition. Scale bar: 100 µm. (c) Wild salmon. Rib showing area of bone resorption in the cortical bone with an intact chondrocyttic core. Note the sparse amount of adipose tissue adjacent to the rib. Scale bar: 500 µm. (d) Wild salmon. Cross section showing rib with adjascent soft tissue facing the abdominal lumen; parietal peritoneum (arrowhead), interstitial connective tissue and elastic fibres. Scale bar: 100 µm. (e) Wild samon. Cross section of rib showing adjacent blood vessel. Scale bar: 100 µm. (f) Farmed salmon. Nerve located in adipose tissue between myocytes adjacent to rib. Scale bar: 100 µm.

the changes and were thus classified as red. In group C, five samples had grade 1, 18 samples had grade 2 and 32 samples had grade 3 MFC. Costal fractures were only detected in five samples by palpation.

3.2 | Radiographic investigations

Radiographic analysis revealed ribs with changes of different types and distribution. The results ranged from no observable changes to ribs with axis deviations, that is, mild bending of axis and distal wave shaped ribs (Figure 1a,b), radiolucent medulla in proximal to mid areas of the ribs (Figure 1c,d), single or multiple costal fractures (Figure 1e), and focal thickening with varying opacity noted as callus formations (Figure 1f). Different costal changes could be detected within the same sample. In group A (no macroscopic discolouration), 9.5% showed costal fractures. Group B (RFC) had a prevalence of 38.4% costal fractures. In group C (MFC), 47,2% of the fillets had fractured ribs. Costal fractures and callus formations were seen only in farmed salmon.

3.3 | Statistical analysis

Statistical analysis was conducted on all radiological findings in relation to macroscopic discolouration. Due to the sample sizes, population 5 was not included in statistical tests on costal changes where the entire length of the rib was required (radiolucent medulla and axis deviations). Ribs with radiolucent medulla and axis deviations were observed in all groups (A, B and C) and showed no statistically significant association with RFC/MFC ($p = >0.05$). In samples with costal fractures and callus formations, discolouration was often present. There was a statistical significant association between costal fractures in fillets detected by radiography, and fillets containing RFC (OR, $p = 0.007$) and MFC (OR, $p = 0.000$). There was no association between callus formations and RFC ($p = >0.05$); however, there was a statistical significant association between MFC and callus formations (OR, $p = 0.000$) found on radiographic investigations.

3.4 | Histological investigations

3.4.1 | Anatomical characteristics of Atlantic salmon ribs

The anatomical characteristics of ribs and adjacent soft tissue were characterised in group A (no macroscopic discolouration). The circumference of the rib was round or oval and smooth or irregular shaped based on the position in question (proximal, mid or distal part) (Figure 2a–g). The ribs displayed a central medullar cavity holding hypertrophic chondrocytes, with layers of a cortical bone

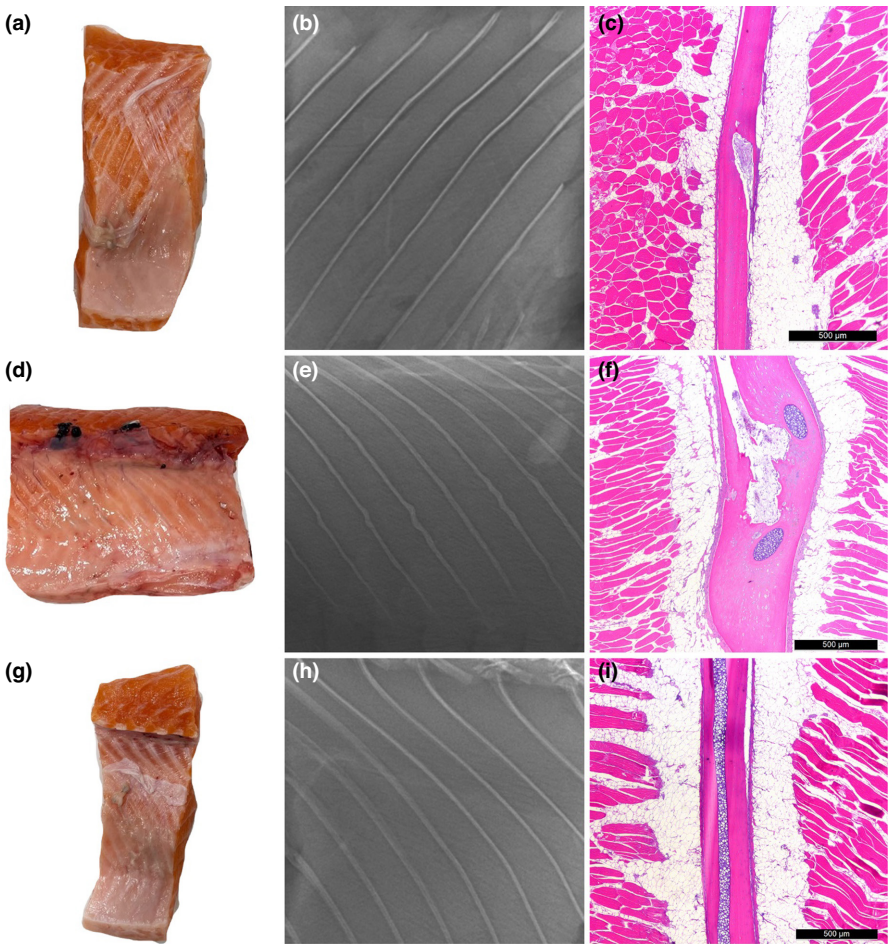

FIGURE 5 Histological investigations of rib changes observed on radiography. Mild bending of rib axis (a-c), distal wave shaped ribs (d-f) and radiolucent medulla (g-i). (a) Macroscopic details of fillet, no discolouration of soft tissue present. (b) Radiographic result of fillet showing mild bending of rib axis. (c) Histological changes of rib with mild bending of axis. Resorption cavity seen in the bone tissue. No pathological changes in surrounding soft tissue. Scale bar: 500 µm. (d) Macroscopic details of fillet, no discolouration of soft tissue present. (e) Radiographic results of fillet showing distal wave shaped ribs. (f) Histological changes of rib with wave shaped appearance. Irregular shaped rib, with the chondrocyttic medulla partly visible in the section. Resorption cavity containing blood vessel seen in a longitudinal direction in rib. No pathological changes in adjacent soft tissue. Scale bar: 500 µm. (g) Macroscopic details of fillet, no discolouration of soft tissue present. (h) Radiographic results of fillet showing ribs with radiolucent medulla. (i) Histological changes of rib with radiolucent medulla. The chondrocyttic medulla and surrounding bone tissue appears intact, no pathological changes in neighbouring soft tissue. Scale bar: 500 µm.

surrounding the centrum (Figure 3a). The bone lamellae were presented with a parallel orientation with no apparent osteons and the bone contained osteocytes embedded in bone matrix (Figure 3b). The cortical bone was covered by periosteum, connective tissue and adipose tissue, with white skeletal muscle tissue adjacent to the proximal and mid part of the ribs (Figure 3a,b). In contrast, distal parts of ribs were surrounded by abundant adipose and connective tissue. In general, wild salmon showed sparse amount of adipose tissue adjacent to the ribs compared to farmed salmon. A cross section of the ribs showed all the structures described above, with chondrocytes in the cartilaginous core (Figure 3c,d). Ribs containing adipose tissue in the medullar cavity were also observed, with central blood vessels in the medullar cavity (Figure 3e,f). At the most distal part of the ribs, chondrocytes in the central medulla appeared to be in a proliferative state (Figure 4a). Several samples showed characteristic changes in the medullar cavity, here described as a *transitional zone*, with resorption of the hyperthrophic chondrocytes and appearance of other cell types, that is, erythrocytes, adipocytes and cellular debris (Figure 4b). In addition, samples could show an intact chondocytic medulla with resorption cavities in the lamellar bone (Figure 4c). Anatomically, as in mammals, the ribs were located in close relation to the peritoneum (Figure 4d) with adjacent vessels and nerves (Figure 4e,f).

3.4.2 | Costal changes – Axis deviations and radiolucent medulla

Due to their occurrence in all groups, ribs with axis deviations and radiolucent medulla on radiography were selected from group A for histological investigations. Mild bending of axis showed no pathological changes in the costal anatomy or surrounding soft tissue

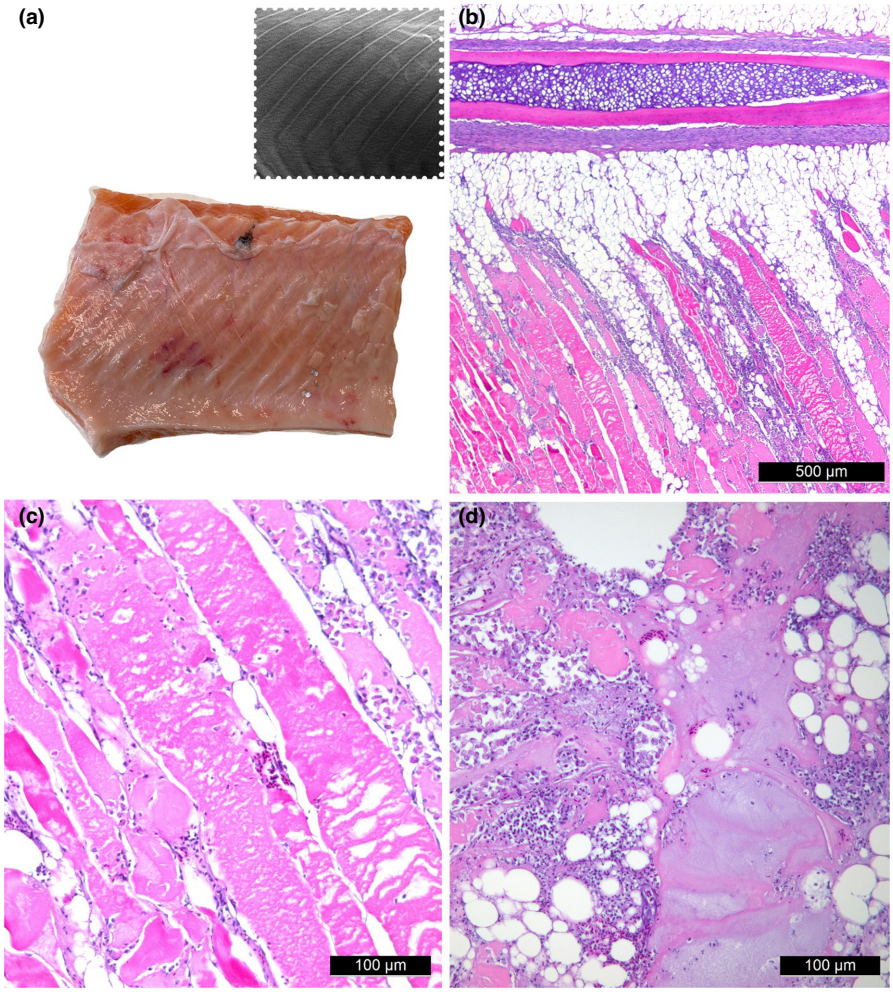

FIGURE 6 Macroscopic, radiographic and histological results of a sample in group B (RFC). (a) Macroscopic evaluation of RFC grade 3 measuring <3 cm, non-pervasive. Stippled square: Radiographic result of area with RFC showing no observable changes in ribs. (b) Histological investigation of area with RFC. No pathological changes in the rib. Neighbouring soft tissue showing degeneration of myocytes and inflammatory cells and haemorrhage. Scale bar: 500 μm. (c, d) Higher magnification (scale bar: 100 μm) of soft tissue inflammation with haemorrhage, degeneration, necrosis and vacuoles present.

(Figure 5a–c). Distal wave shaped ribs were difficult to evaluate in sections, as the rib axis deviated in both lateral/medial and cranial/caudal direction. Nevertheless, the microscopic anatomy of wave shaped ribs was identical to that described in Figure 4a, with proliferative chondrocytes in the medullar cavity (Figure 5d–f). Ribs with radiolucent medulla (Figure 5g,i) on radiography had either a chondrocyttic or an adipocytic medullar cavity, with occational resorption cavities as seen in Figure 4c. No pathological changes were observed in the neighbouring soft tissue.

3.4.3 | Ribs in relation to red focal changes

The histological characteristics of RFC were in line with previous reports (Bjørgen et al., 2015, 2019, 2020), with mild to severe haemorrhage in the soft tissue, necrosis and degeneration of myocytes and infiltration of inflammatory cells. Such findings were not consistently found associated with costal changes (Figure 6a). Herein, affection solely of the adjacent soft tissue at the level of the rib was observed (Figure 6b–d). Other samples contained costal fractures located in the area of the RFC (Figure 7a) but with no affection of the neighbouring soft tissue following histological examination (Figure 7b). Grade 3 RFC could be found without severe costal changes (Figure 7c,d).

3.4.4 | Ribs in relation to melanized focal changes

Group C contained samples of MFC graded from 1 to 3 macroscopically. In radiological investigations, 26 of 55 samples had costal fractures. Sections retrieved from areas containing MFC revealed several different changes histologically, ranging from no histological changes in the bone tissue or neighbouring soft tissue to severe structural changes in both. Histological changes in the soft tissue corresponded to the findings and classification of MFC done by Bjørgen et al. (2019), with changes ranging from mild inflammation and sparse presence of melano-macrophages in the soft tissue to complete loss of skeletal muscle architecture and abundant presence of melano-macrophages, granulomas, fibrosis and inflammation.

As in group B, MFC could have no costal changes on radiology or histology (Figure 8a,b); however, in the adipose tissue of the myosepta near the ribs, melano-macrophages were often found between adipocytes and vessels (Figure 8c,d). Analysis of ribs in MFC could also have similar resorption patterns as seen in samples from group A (Figure 9a–d), but with no apparent affection of the adjacent soft tissue.

When examined by histology, radiographically detected fractures occasionally displayed callus-like structures (Figure 10a–c). Distinct fractures were also observed (Figure 10d–f). These

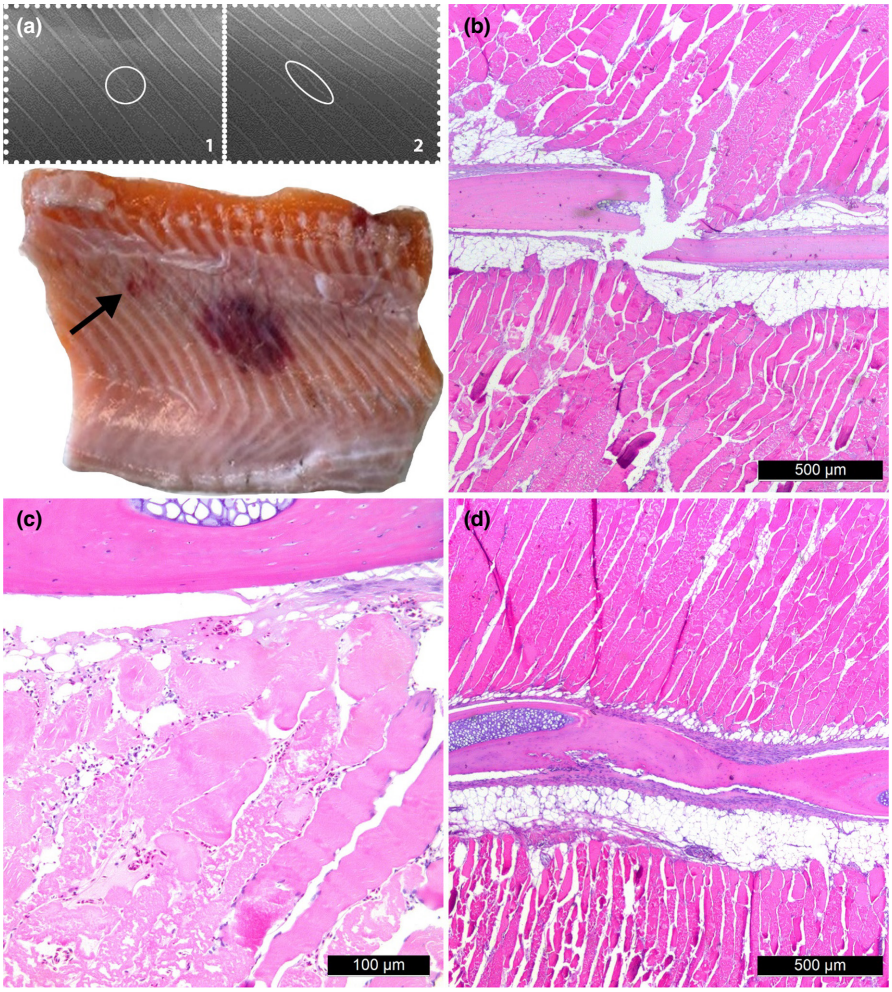

FIGURE 7 Macroscopic, radiographic and histological results of a sample in group B (RFC). (a) Macroscopic evaluation of RFC grade 2 measuring >1 cm (arrow) and RFC grade 3 measuring >3 cm, non-pervasive. Stippled square 1: Radiographic result of RFC grade 2 showing costal fracture (circle). Stippled square 2: Radiographic result of RFC grade 3 showing rib with axis deviation (oval). (b) Histological findings in rib located in area of RFC grade 2. Costal fracture, with no apparent affection of the surrounding soft tissue. Scale bar: 500 μm. (c) Histological findings in RFC grade 3, showing area of soft tissue adjacent to a radiological normal rib with haemorrhage between myocytes and infiltrating inflammatory cells. Degenerated myocytes. Scale bar: 100 μm. (d) Histological findings in rib with axis deviation located in area of RFC grade 3, with no pathological changes in bone structure or in the chondrocyttic core. Adjacent soft tissue is intact. Scale bar: 500 μm.

changes did not consistently correlate with the severity of the MFC (Figure 10d–f); however, samples with grade 3 MFC often showed severe changes in both ribs and adjacent soft tissue (Figure 10g–i). Callus formations were histologically seen as focal thickening of unorganised bone with resorption cavities (Figure 11a–d). Presence of melano-macrophages in adjacent soft tissue was often evident.

4 | DISCUSSION

The rationale for this study was to describe anatomical characteristics of ribs in the Atlantic salmon, and to apply this information in investigating different pathological changes affecting the ribs, and finally, to identify the possible association between costal changes and RFC/MFC. Thus, novel anatomical information provided a basis for the interpretation of different costal changes. Samples of the lateral musculature including ribs were obtained from different groups of Atlantic salmon (wild, farmed and hybrids). The material was categorised by macroscopic evaluation into three different groups: Group A (no macroscopic discolouration), group B (red focal changes/RFC) and group C (melanized focal changes/MFC). All groups were investigated by macroscopical, radiographical and histological analysis.

The samples in all groups were radiographed to reveal possible associations between macroscopic discolouration and costal changes. The variations in rib morphology detected by radiographic investigations coincided with the results of Jiménez-Guerrero et al. 2022 and other radiographic investigations on teleost fish (Fjelldal et al., 2020). As both longitudinal radiolucent ribs and axis variations, that is, mild bending and distal wave shape, were observed in all groups, we assume these costal variations to be of non-pathological nature. Thus, such costal variations detected in fish with macroscopic discolouration and/or inflammation in adjacent soft tissue could be a coincidental finding. Costal fractures and callus formations were commonly found in relation to MFC, indicating that such changes may cause MFC. Alternatively, the chronic inflammatory environment in the neighbouring soft tissue may cause the costal bone tissue to deteriorate, leading to altered rib morphology.

In our study, 40 samples were classified with costal fractures by radiographic examination. Costal fractures were only seen in fish kept in captivity, that is, in on-land tanks and sea water cages. Our results suggest that the cause of costal fractures may lie in the rearing conditions (handling, nutrition etc.), or in the genetic differences between farmed and wild fish (Gjedrem et al., 1991; Gjøen & Bentsen, 1997). However, our wild fish material was limited, and six of ten wild fish samples were not radiographed. Other reports

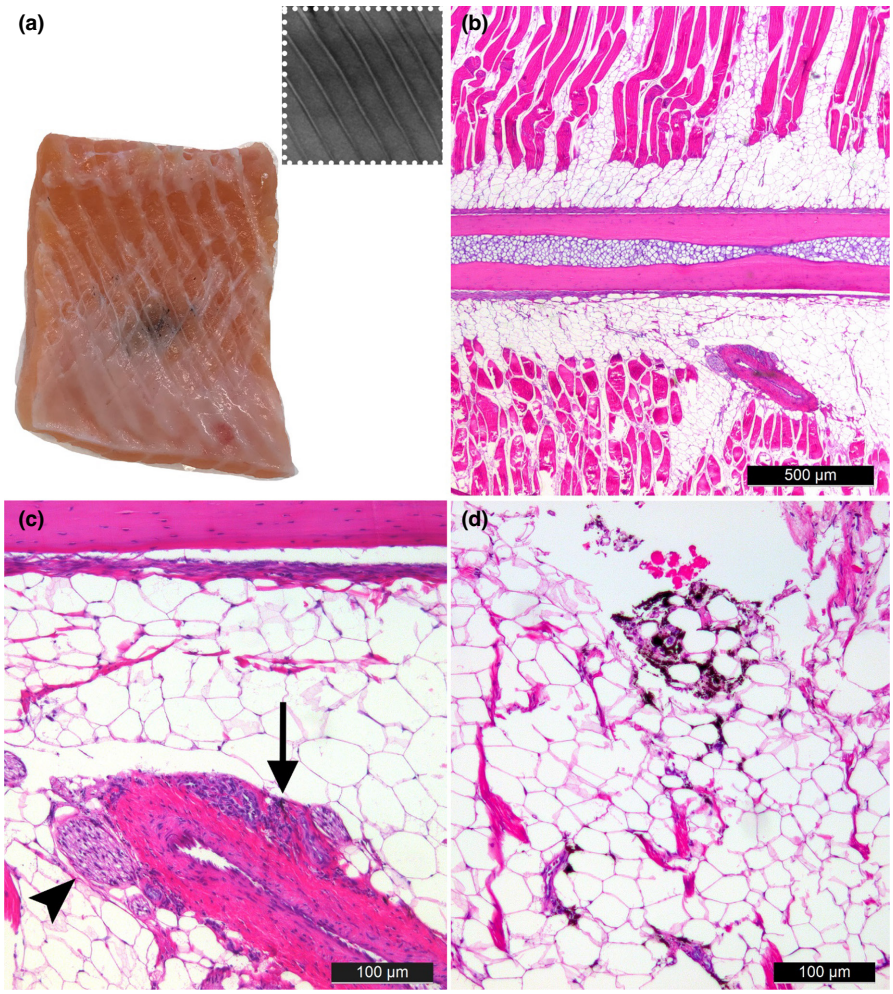

FIGURE 8 Macroscopic, radiographic and histological results of a sample in group C (MFC). (a) Macroscopic evaluation of MFC grade 2, measuring 2 cm, >1 cm deep, non-pervasive. Stippled square: Radiographic results with no observable costal changes. (b) Histological results of area containing MFC. No pathological findings in rib or adjacent soft tissue. A vessel and a nerve are located in close relation to the rib. Scale bar: 500 μm. (c) Vessel and nerve (arrowhead). Melano-macrophages (arrow) in relation to vessel. Scale bar: 100 μm. (d) Melano-macorphages surrounding vacuoles and a vessel in the myoseptal adipose tissue in the area above the rib, towards the peritoneal cavity. Scale bar: 100 μm.

on the prevalence of bone fractures in reared versus wild fish show conflicting results with costal fractures occurring in wild fish (Fjelldal et al., 2020; Jiménez-Guerrero et al., 2022). In commercial aquaculture, skeletal deformities are common and may affect the fish's ability to swim, eat and consequently grow and survive. It is thus of interest to uncover the prevalence and cause of costal fractures, both for animal welfare and production-related interests. As an initial cause of costal fractures in general, trauma is a common and plausible explanation. Incautious rearing conditions may imply rough handling causing local trauma. However, the salmon ribs are well positioned in the myosepta, and the breaking force is expected to be high. Investigations on the mechanical properties of farmed Atlantic salmon ribs showed an increased breaking force following an increase in body weight, pointing out the proximal part of the anterior ribs as the most resistant to breakage (Yao & Mørkøre, 2017). By comparison, farmed rainbow trout showed rib thickness (mm) smaller than that of salmon, but the breaking force is reported to be higher. In this context, it should be noted that the prevalence of MFC in farmed rainbow trout is much lower than in farmed salmon, although most farming conditions are similar (Bjørgen et al., 2015; Mørkøre et al., 2015; Olsen et al., 2021). One other possible scenario is that the force that causes the costal fracture and muscle damage originates from within the abdominal cavity. Following this notion, the ribs of rainbow trout could be strong and stiff enough to protect the underlying musculature, while the weaker and softer ribs of Atlantic salmon could bend and break or bend without fracture, both resulting in a local muscle edema caused by restricted blood flow or bleeding caused by fracture. Such forces could be caused by the swelling of the formulated dry pellets fed to farmed Atlantic salmon, which drinks seawater as part of their natural hypo-osmoregulation (Usher et al., 1988).

As ribs are in close proximity to RFC/MFC, costal changes could be an initial cause of RFC and ultimately MFC. This has recently been addressed by Jiménez-Guerrero et al. (2022). By investigating fillets both with and without macroscopic discolouration, we sought to differentiate costal changes related to discolouration, and changes found in all groups, suggesting the latter being normal variations. Association was not detected between macroscopic discolouration and radiolucent medulla and axis deviations. A statistically significant association was found between RFC/MFC and costal fractures detected by radiographic investigations. However, as histological investigations revealed unaffected ribs in the area of the RFC, and vice versa, these findings underline the importance of histological investigations. MFC were also occasionally found without costal changes, thus the underlying cause of macroscopic discolouration cannot be explained by costal fractures alone.

As with costal fractures, focal bone thickening noted as callus formations were only found in salmon held in captivity. In earlier

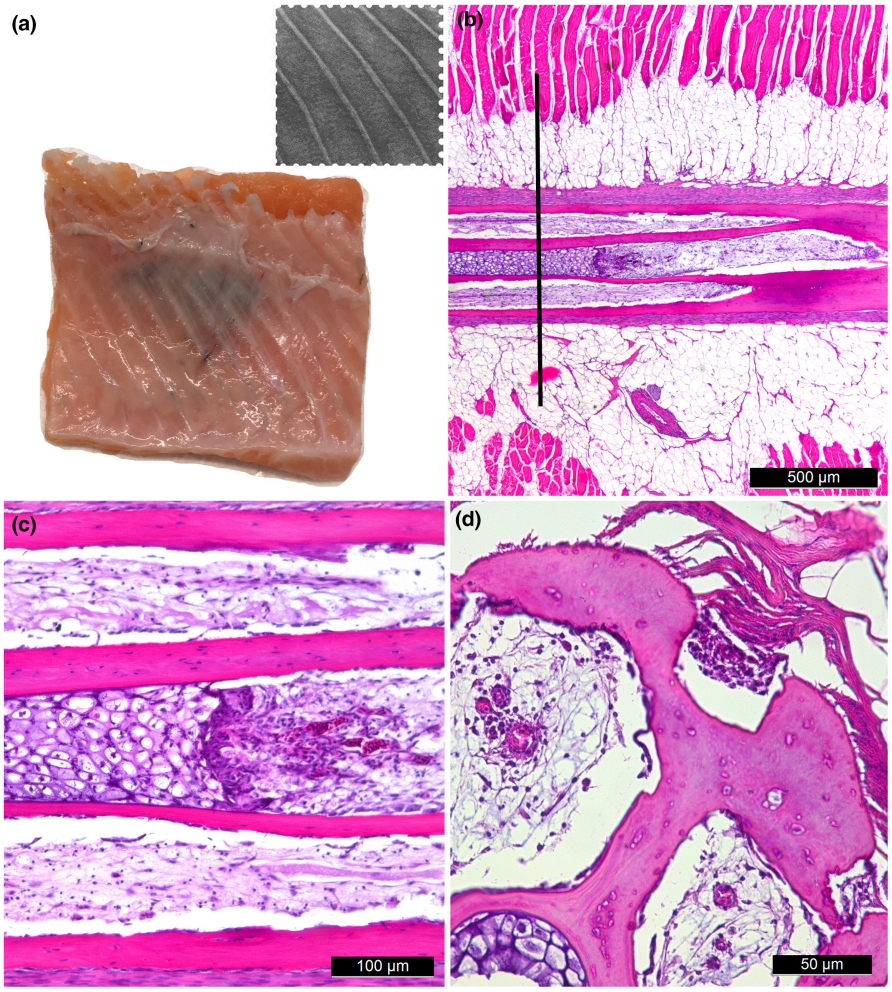

FIGURE 9 Macroscopic, radiographical and histological investigation of a sample in group C (MFC). (a) MFC in sample measuring >3 cm, 2 cm deep, pervasive. Stippled square: Radiographic results of ribs in area of the MFC showing radiolucent medulla in mid part of ribs. (b) Histological characteristics of rib with radiolucent appearance. No pathological changes in surrounding soft tissue. Central medulla of rib showing a transitional zone with removal of hyperthropic chondrocytes. Cavities in the cortical bone adjacent to central medulla showing similar components as the transferred central cavity. Black line: Marked area of cross section in 'd'. Scale bar: 500 μm. (c) Central chondrocyttic medulla with transitional zone. Erythrocytes present post transition. Scale bar: 100 μm. (d) Cross section of area marked with a black line in 'b' showing vessels containing erythrocytes in cavities adjacent to an intact chondrocyttic medulla. Scale bar: 50 μm.

reports, findings of focal bone thickening in teleost bones have been noted as hyperostosis, or swollen bone. Based on several observations, such as species-specific patterns and onset timing of development, hyperostosis in teleosts is regarded a non-pathological expansion of bone (Smith-Vaniz et al., 1995). However, a possible link between hyperostosis and bone fractures has been suggested (Fjelldal et al., 2018, 2020; Jawad, 2013). Fjelldal et al. (2020) discovered a high prevalence of site-specific hemal and neural spine callus-like formations in the axial skeleton in wild ballan wrasse (*Labrus bergylta*), similar to the callus formations in our samples, herein suggesting that a continuous mechanical load may cause the bone to fracture followed by a fracture healing process. Due to the sampling method in our study, we were not able to pinpoint the specific rib (number) in question, as the samples were cropped to include a limited area of the axial skeleton. Thus, site-specific findings were not included in our work. Also, as the size of the hyperostotic structures varies among species and individuals, these structures could in some cases be challenging to distinguish from callus formation only using radiographic investigations. However, due to the association between callus formations and MFC found in our work, it is likely that these changes are the result of a pathological condition in the bone tissue.

By histological investigations, we were able to show anatomical characteristics of Atlantic salmon ribs coinciding with findings in earlier reports, such as osteocyttic bone, longitudinal bone lamella and a chondrocyttic or adipocytic medulla. A transition zone was noted in several ribs. In both wild and farmed fish, multiple longitudinal vessels were found in the adipocyttic medulla post cartilage resorption, and within resorption cavities in the cortical bone with the chondrocyttic core still intact. To our knowledge, such vascularisation of teleost ribs has not been previously described. Resorption cavities in the cortical bone were found both in ribs presented as normal on radiographic investigations, but also in ribs presented with axis deviations and radiolucent medulla. The latter corresponds well with micro-CT results done on thickened salmon rib, herein revealing a thinner compacta with resorptive appearance (Jiménez-Guerrero et al., 2022). As in mammals, bone resorption and vascularisation of bony tissue is a vital part of the bone development and remodelling in teleosts (Benzinou et al., 2002), and resorption activity of both mono- and multinucleated osteoclasts in teleost fish has been well reviewed by Witten and Huysseune (Witten & Huysseune, 2009). In carp and tilapia, Cohen et al. (2012) described an area of woven-like bone structure in the central part of the rib with occasional perforation by the central lumina (Cohen et al., 2012). Interestingly, fish with acellular bone has shown an increase of the hollow medullar cavity correlated with an increase of stiffness of the rib (Horton & Summers, 2009), as is the case in mammals and birds. This might indicate that the resorption of bone in our results is in fact making the

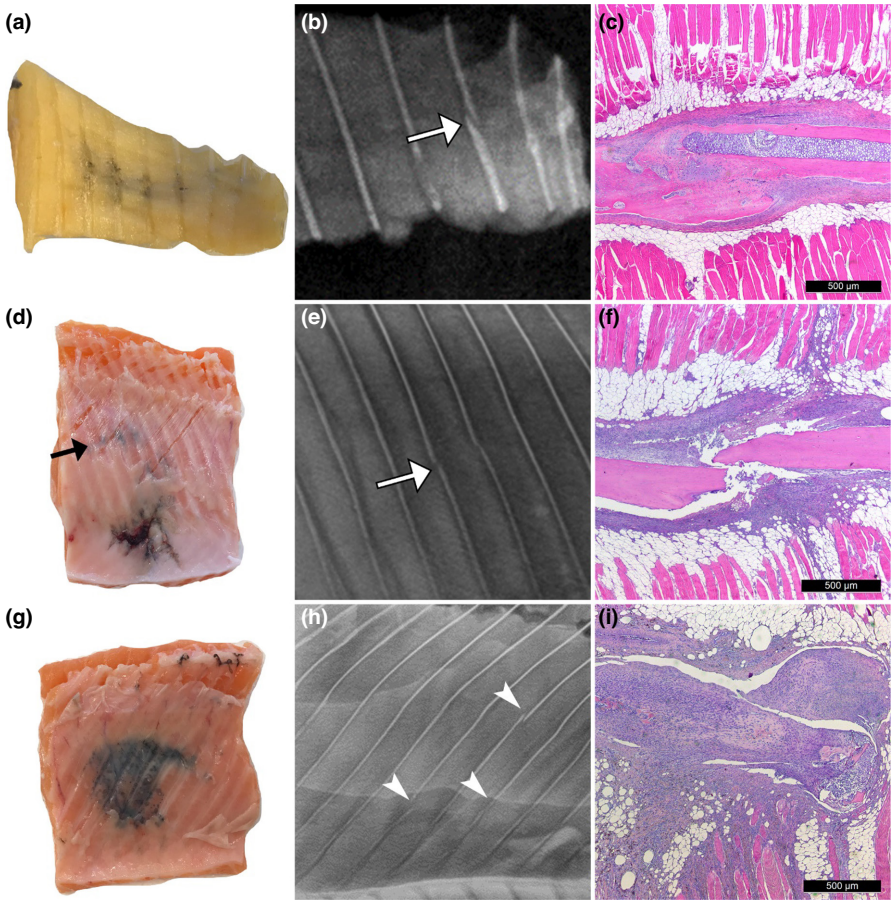

FIGURE 10 Macroscopic, radiographic and histological results of samples in group C (MFC). (a) Macroscopic evaluation of MFC grade 2, measuring >2 cm. (b) Radiographic result of sample in 'a', showing costal fracture (arrow). (c) Histological characteristics of costal fracture seen in 'b'. Loss of normal rib structure, callus-like formation surrounding rib bone collar with an irregular appearance of the longitudinal section of rib. No resorption cavities. No affection of neighbouring soft tissue. Scale bar: 500 μm. (d) Macroscopic evaluation of MFC grade 3, measuring >3 cm, non-pervasive and MFC grade 2, measuring <2 cm (arrow). (e) Radiographic results of sample in 'd', showing costal fracture (arrow). (f) Histological characteristics of costal fracture seen in 'e'. Costal fracture with inflammatory cells present in soft tissue. Adjacent myocytes are degenerated, and melano-macrophages and vacuoles are present in the area of inflammation. Scale bar: 500 μm. (g) Macroscopic evaluation MFC grade 3, measuring >3 cm, 2 cm deep, non-pervasive. (h) Radiographic results of sample in 'g', showing costal fractures (arrowheads). (i) Histological investigations of area containing costal fractures in 'h'. Total loss of normal tissue arcitecture in rib and adjacent soft tissue. Inflammatory cells are present, in addition to melano-macrophages and vacuoles. Degeneration of myocytes is evident. Scale bar: 500 μm.

rib more resistant by adapting to changing stressors, a trait beneficial to the fish. If so, this corresponds to the increased breaking force following increased body weight (Yao & Mørkøre, 2017). However, it is noteworthy that cross sections of the ribs revealed an irregular appearance of the outer circumference in addition to large resorption cavities in the bone, resulting in areas of distinctly thinner cortical bone. There is limited knowledge on osteoporosis in farmed Atlantic salmon; however, osteoporotic conditions can be induced by several factors in teleost species such as zebrafish (Rosa et al., 2021), a fish widely utilized in research revolving human medicine. We speculate if the resorptive changes in Atlantic salmon rib are pathologically induced, thus affecting the rib breaking force negatively, or if this is merely a physiological and anatomical trait in salmon due to life in an aquatic milieu.

Co-occurring resorption and bone formation is vital for healthy bone growth, thus as the fish grows, bones will subsequently increase in size. Ribs with radiographical radiolucent medulla were detected in all groups, but not in all samples. As these findings were often located in proximal and mid parts of the ribs, we speculate that the increased thickness of the rib due to growth is what allows the X-ray beam to pass through tissue that are of less radiopaque properties, giving the medulla a radiolucent appearance. The size of the individual fish was not registered in our work; however, we believe that the fish size will impact the findings of radiolucent medulla.

Histological investigations of the most distal part of ribs, both normal and wave shaped ribs, revealed a central medulla containing proliferative chondrocytes. These results are in line with Soliman (2018), showing chondrocytes arranged as resting, proliferating and hypertrophic zones in the medullar cavity in both the proximal and distal part of the rib. In our work, we were not able to reveal a proximal growth plate in the ribs. Wave shaped ribs were solely located at the distal end of the rib, surrounded by abundant

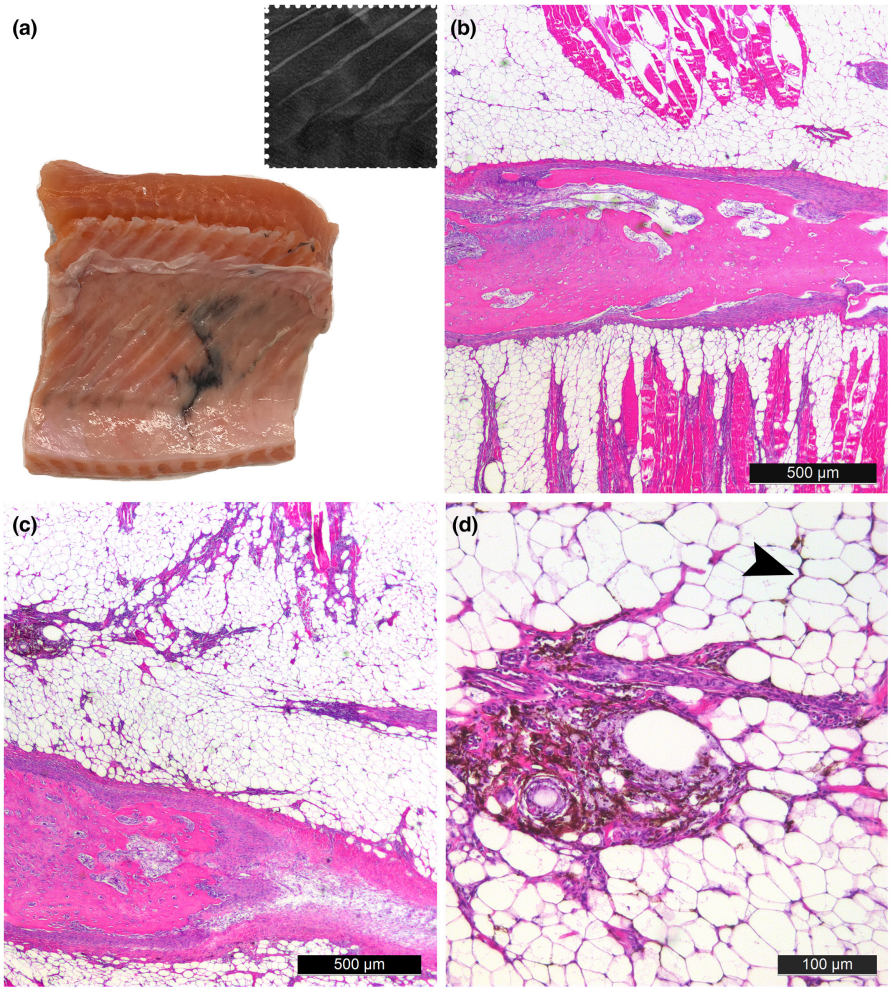

FIGURE 11 Macropscopic, radiographical and histological investigation of a sample in group C (MFC) presented with focal thickening of ribs detected on radiographic investigations. (a) MFC measuring >3 cm in length, non-pervasive. Stippled square: Radiographic results showing thickened, irrgular shape in distal regions of ribs. (b) Histological findings in thickened and irregular rib located in area of melanized focal change. Normal bone tissue arcitecture is lacking, with focal bone resorption. Adjacent soft tissue with infiltrating inflammatory cells and vacuoles. Scale bar: 500 µm. (c) Adjacent soft tissue dominated by adipocytes, with melano-macrophages present. Scale bar: 500 µm. (d) Granuloma with abundant presence of surrounding melano-macrophages. Melano-macrophages are also present between adipocytes (arrowhead). Scale bar: 100 µm.

adipose tissue and to a lesser extent skeletal muscle tissue. We speculate that this axis deviation is due to the anatomical structure and position, as muscle attachment surely will anchor the ribs and restrict their shape in more proximal areas; however, ribs noted as wiggled have also been observed in Atlantic salmon with phosphorus deficiency (Baeverfjord et al., 1998). No pathological changes were found in the cortical bone or surrounding soft tissue of wave shaped ribs in group A; however, in samples with MFC located at the equivalent areas, neighbouring soft tissue could be severely affected. In terms of other axis deviations, histological investigations on mild bending of axis in group A revealed normal bone morphology and surrounding soft tissue, with a mild curve in the rib axis. Thus, supported by radiology and statistics, both axis deviations found in our work are suggested to be normal variations of rib morphology in at least some teleost species, including Atlantic salmon. However, these results cannot rule out that inflammation in the soft tissue can alter the axis of the rib, or that these deviations show different breaking force than other costal changes, as resorption of the cortical bone followed by vascularization was indeed seen in all parts of the rib, including the distal wave shaped part.

As Moss pointed out in 1961 (Moss, 1961), the vascular pattern in teleost bone varies substantially among species and even within one individual. Our findings show several longitudinal vessels within the ribs, thus the ribs in Atlantic salmon have great potential for haemorrhage and the recruiting of haematopoietic and inflammatory cells in the event of a fracture. The histological investigations conducted in our study showed that costal fractures could be accompanied by acute inflammation and haemorrhage in the adjacent muscle and connective tissue. This complies with mammalian fracture repair explained by a four-stage model, where a fracture will cause haemorrhage in the neighbouring soft tissue, followed by acute inflammation, callus formation and remodelling of the callus (Kolar et al., 2011; Marsell & Einhorn, 2011; Schindeler et al., 2008). In Moss' work on fracture repair in acellular and cellular teleosts (Moss, 1962), the examined opercular and lower jaw elements were sparsely vascularised, thus a hematoma was not a dominating feature in the fracture healing process. In our work, costal fractures were occasionally found with no changes in the neighbouring soft tissue, indicating that the fracture occurred postmortem. Importantly, some samples with focal macroscopic discolouration contained costal fractures in the equivalent area presented by radiography; however, histological investigations revealed postmortem fractures, thus the macroscopic focal discolouration herein must have a different origin.

In mammalian fracture healing, bone splints are covered by a soft and later a hard callus. We show that ribs with callus-like appearance in radiology were histologically presented with corresponding callus

properties, that is, woven bone with resorption cavities covering areas of what was presumed to be an old fracture site. This is in line with earlier reports on fracture healing in teleosts using both radiography and histology (Fjelldal et al., 2018; Geurtzen et al., 2014; Moss, 1962; Takeyama et al., 2014).

In sum, our study has shown variations in the anatomical characteristics in Atlantic salmon ribs, including vascularisation and resorption cavities. This included ribs with intact chondrocyttic medulla and no vessels or resorption cavities present, and ribs with multiple longitudinal vessels in both the medullar cavity and in resorption cavities in the cortical bone. Our results provide additional knowledge to the association between costal changes and RFC/MFC found in earlier reports and has demonstrated the potential for local haemorrhage in the event of costal fractures. In accordance with earlier findings, the initial cause of RFC/MFC cannot be fully explained by costal changes alone.

ACKNOWLEDGEMENTS

The Norwegian Seafood Research Fund (FHF) is acknowledged for funding (Grant number 901501). Ms. Clementine Linde is acknowledged for valuable laboratory assistance.

CONFLICT OF INTEREST

The authors declare no conflicts of interest.

DATA AVAILABILITY STATEMENT

The data that support the findings of this study (histological slides and X-ray files) are available from the corresponding author upon reasonable request.

ORCID

Håvard Bjørgen https://orcid.org/0000-0003-4683-0088

REFERENCES

Aunsmo, A., Guttvik, A., Midtlyng, P. J., Larssen, R. B., Evensen, Ø., & Skjerve, E. (2008). Association of spinal deformity and vaccine-induced abdominal lesions in harvest-sized Atlantic salmon, *Salmo salar* L. *Journal of Fish Diseases*, *31*(7), 515–524. https://doi.org/10.1111/j.1365-2761.2007.00899.x

Baeverfjord, Aasgaard, T. E., & Shearer, K. (1998). Development and detection of phosphorus deficiency in Atlantic salmon, *Salmo salar* L., parr and post-smolts. *Aquaculture Nutrition*, *4*(1), 1–11. https://doi.org/10.1046/j.1365-2095.1998.00095.x

Benzinou, A., Casselman, J. M., Folkvord, A., Geffen, A. J., Troadec, H., McCurdy, W. J., Mesnil, B., Meunier, F. J., Moksness, E., Morales-Nin, B., Mosegaard, H., Panfili, J., de Pontual, H., Troadec, H., & Wright, P. J. (2002). *Manuel de sclérochronologie des poissons*. Ifremer.

Bjørgen, H., Haldorsen, R., Oaland, Ø., Kvellestad, A., Kannimuthu, D., Rimstad, E., & Koppang, E. O. (2019). Melanized focal changes in skeletal muscle in farmed Atlantic salmon after natural infection with *piscine orthoreovirus* (PRV). *Journal of Fish Diseases*, *42*(6), 935–945. https://doi.org/10.1111/jfd.12995

Bjørgen, H., & Koppang, E. O. (2021). Anatomy of teleost fish immune structures and organs. *Immunogenetics*, *73*(1), 53–63. https://doi.org/10.1007/s00251-020-01196-0

Bjørgen, H., Kumar, S., Gunnes, G., Press, C. M., Rimstad, E., & Koppang, E. O. (2020). Immunopathological characterization of red focal changes in Atlantic salmon (*Salmo salar*) white muscle. *Veterinary Immunology and Immunopathology*, *222*, 110035. https://doi.org/10.1016/j.vetimm.2020.110035

Bjørgen, H., Wessel, Ø., Fjelldal, P. G., Hansen, T., Sveier, H., Sæbø, H. R., Enger, K. B., Monsen, E., Kvellestad, A., Pimstad, E., & Koppang, E. O. (2015). *Piscine orthoreovirus* (PRV) in red and melanised foci in white muscle of Atlantic salmon (*Salmo salar*). *Veterinary Research*, *46*, 89. https://doi.org/10.1186/s13567-015-0244-6

Boglione, C., Gavaia, P., Koumoundouros, G., Gisbert, E., Moren, M., Fontagné, S., & Witten, P. E. (2013). Skeletal anomalies in reared European fish larvae and juveniles. Part 1: Normal and anomalous skeletogenic processes. *Reviewa in Aquaculture*, *5*(s1), S99–S120. https://doi.org/10.1111/raq.12015

Boglione, C., Pulcini, D., Scardi, M., Palamara, E., Russo, T., & Cataudella, S. (2014). Skeletal anomaly monitoring in rainbow trout (*Oncorhynchus mykiss*, Walbaum 1792) reared under different conditions. *PLoS One*, *9*(5), e96983. https://doi.org/10.1371/journal.pone.0096983

Cohen, L., Dean, M., Shipov, A., Atkins, A., Monsonego-Ornan, E., & Shahar, R. (2012). Comparison of structural, architectural and mechanical aspects of cellular and acellular bone in two teleost fish. *The Journal of Experimental Biology*, *215*(11), 1983–1993. https://doi.org/10.1242/jeb.064790

Darias, M. J., Mazurais, D., Koumoundouros, G., Cahu, C. L., & Zambonino-Infante, J. L. (2011). Overview of vitamin D and C requirements in fish and their influence on the skeletal system. *Aquaculture*, *315*(1), 49–60. https://doi.org/10.1016/j.aquaculture.2010.12.030

Davesne, D., Meunier, F. J., Schmitt, A. D., Friedman, M., Otero, O., & Benson, R. B. J. (2019). The phylogenetic origin and evolution of acellular bone in teleost fishes: Insights into osteocyte function in bone metabolism. *Biological Reviews*, *94*(4), 1338–1363. https://doi.org/10.1111/brv.12505

de Haan, D., Fosseidengen, J. E., Fjelldal, P. G., Burggraaf, D., & Rijnsdorp, A. S. (2016). Pulse trawl fishing: Characteristics of the electrical stimulation and the effect on behavior and injuries of Atlantic cod (*Gadus morhua*). *ICES Journal of Marine Science*, *73*(6), 1557–1569. https://doi.org/10.1093/icesjms/fsw018

Debes, P. V., Solberg, M. F., Matre, I. H., Dyrhovden, L., & Glover, K. A. (2021). Genetic variation for upper thermal tolerance diminishes within and between populations with increasing acclimation temperature in Atlantic salmon. *Heredity*, *127*(5), 455–466. https://doi.org/10.1038/s41437-021-00469-y

Eriksen, M. S., Bakken, M., Espmark, Å., Braastad, B. O., & Salte, R. (2006). Prespawning stress in farmed Atlantic salmon *Salmo salar*: Maternal cortisol exposure and hyperthermia during embryonic development affect offspring survival, growth and incidence of malformations. *Journal of Fish Biology*, *69*(1), 114–129. https://doi.org/10.1111/j.1095-8649.2006.01071.x

Fjelldal, P. G., Hansen, T., Breck, O., Ørnsrud, R., Lock, E. J., Waagbø, R., Wargelius, A., & Witten, P. E. (2012). Vertebral deformities in farmed Atlantic salmon (*Salmo salar* L.) – Etiology and pathology. *Journal of Applied Ichthyology*, *28*(3), 433–440. https://doi.org/10.1111/j.1439-0426.2012.01980.x

Fjelldal, P. G., Madaro, A., Hvas, M., Stien, L. H., Oppedal, F., & Fraser, T. W. (2020). Skeletal deformities in wild and farmed cleaner fish species used in Atlantic salmon *Salmo salar* aquaculture. *Journal of Fish Biology*, *98*(4), 1049–1058. https://doi.org/10.1111/jfb.14337

Fjelldal, P. G., van der Meeren, T., Fraser, T. W. K., Sambraus, F., Jawad, L., & Hansen, T. J. (2018). Radiological changes during fracture and repair in neural and haemal spines of Atlantic cod (*Gadus morhua*). *Journal of Fish Diseases*, *41*(12), 1871–1875. https://doi.org/10.1111/jfd.12899

Geurtzen, K., Knopf, F., Wehner, D., Huitema, L. F. A., Schulte-Merker, S., & Weidinger, G. (2014). Mature osteoblasts dedifferentiate in response to traumatic bone injury in the zebrafish fin and skull.

Development, *141*(11), 2225–2234. https://doi.org/10.1242/dev.105817

Gil Martens, L., Lock, E. J., Fjelldal, P. G., Wargelius, A., Araujo, P., Torstensen, B. E., Witten, P. E., Hansen, T., Waagbø, R., & Ørnsrud, R. (2010). Dietary fatty acids and inflammation in the vertebral column of Atlantic salmon, *Salmo salar* L., smolts: A possible link to spinal deformities. *Journal of Fish Diseases*, *33*(12), 957–972. https://doi.org/10.1111/j.1365-2761.2010.01201.x

Gislason, H., Karstensen, H., Christiansen, D., Hjelde, K., Helland, S., & Bæverfjord, G. (2010). Rib and vertebral deformities in rainbow trout (*Oncorhynchus mykiss*) explained by a dominant-mutation mechanism. *Aquaculture*, *309*(1), 86–95. https://doi.org/10.1016/j.aquaculture.2010.09.016

Gjedrem, T., Salte, R., & Gjøen, H. M. (1991). Genetic variation in susceptibility of Atlantic salmon to furunculosis. *Aquaculture*, *97*(1), 1–6. https://doi.org/10.1016/0044-8486(91)90274-B

Gjøen, H. M., & Bentsen, H. B. (1997). Past, present, and future of genetic improvement in salmon aquaculture. *ICES Journal of Marine Science*, *54*(6), 1009–1014. https://doi.org/10.1016/S1054-3139(97)80005-7

Horton, J. M., & Summers, A. P. (2009). The material properties of acellular bone in a teleost fish. *Journal of Experimental Biology*, *212*(Pt 9), 1413–1420. https://doi.org/10.1242/jeb.020636

Jawad, L. A. (2013). Hyperostosis in three fish species collected from the sea of Oman. *American Association for Anatomy*, *296*(8), 1145–1147. https://doi.org/10.1002/ar.22728

Jiao, Y. Y., Okada, M., Hara, E. S., Xie, S. C., Nagaoka, N., Nakano, T., & Matsumoto, T. (2020). Micro-architectural investigation of teleost fish rib inducing pliant mechanical property. *Materials*, *13*(22), 5099. https://doi.org/10.3390/ma13225099

Jiménez-Guerrero, R., Baeverfjord, G., Evensen, Ø., Hamre, K., Larsson, T., Dessen, J.-E., Gannestad, K.-H., & Mørkøre, T. (2022). Rib abnormalities and their association with focal dark spots in Atlantic salmon fillets. *Aquaculture*, *561*, 738697. https://doi.org/10.1016/j.aquaculture.2022.738697

Kague, E., Hughes, S. M., Lawrence, E. A., Cross, S., Martin-Silverstone, E., Hammond, C. L., & Hinits, Y. (2019). Scleraxis genes are required for normal musculoskeletal development and for rib growth and mineralization in zebrafish. *Federation of American Societies for Experimental Biology*, *33*(8), 9116–9130. https://doi.org/10.1096/fj.201802654RR

Kolar, P., Gaber, T., Perka, C., Duda, G. N., & Buttgereit, F. (2011). Human early fracture hematoma is characterized by inflammation and hypoxia. *Clinical Orthopaedics and Related Research*, *469*(11), 3118–3126. https://doi.org/10.1007/s11999-011-1865-3

Kölliker, A. (1857). On the different types in the microscopic structure of the skeleton of osseous fishes. *Proceedings of the Royal Society of London*, *9*, 656–668. https://doi.org/10.1098/rspl.1857.0132

Koppang, E. O., Haugarvoll, E., Hordvik, I., Aune, L., & Poppe, T. T. (2005). Vaccine-associated granulomatous inflammation and melanin accumulation in Atlantic salmon, *Salmo salar* L., white muscle. *Journal of Fish Diseases*, *28*(1), 13–22. https://doi.org/10.1111/j.1365-2761.2004.00583.x

Kryvi, H., & Poppe, T. (2016). *Fiskeanatomi*. Fagbokforlaget.

Larsen, H. A. S., Austbø, L., Mørkøre, T., Thorsen, J., Hordvik, I., Fischer, U., Jirillo, E., Rimstad, E., & Koppang, E. O. (2012). Pigment-producing granulomatous myopathy in Atlantic salmon: A novel inflammatory response. *Fish Shellfish Immunology*, *33*(2), 277–285. https://doi.org/10.1016/j.fsi.2012.05.012

Loi, F., Córdova, L. A., Pajarinen, J., Lin, T.-H., Yao, Z., & Goodman, S. B. (2016). Inflammation, fracture and bone repair. *Bone*, *86*, 119–130. https://doi.org/10.1016/j.bone.2016.02.020

Marsell, R., & Einhorn, T. A. (2011). The biology of fracture healing. *Injury*, *42*(6), 551–555. https://doi.org/10.1016/j.injury.2011.03.031

Martini, A., Huysseune, A., Witten, P. E., & Boglione, C. (2021). Plasticity of the skeleton and skeletal deformities in zebrafish (*Danio rerio*) linked to rearing density. *Journal of Fish Biology*, *98*(4), 971–986. https://doi.org/10.1111/jfb.14272

Mørkøre, T., Larsson, T., Kvellestad, A. S., Koppang, E. O., Åsli, M., Krasnov, A., Dessen, J.-E., Moreno, H. M., Valen, E., Gannestad, K. H., Gjerde, B., Taksdal, T., Bæverfjord, G., Meng, Y., Heia, K., Wold, J. P., Borderias, A. J., Moghadam, H., Romarheim, O. H., & Rørvik, K.-A. (2015). *Mørke flekker i laksefilet. Kunnskapsstatus og tiltak for å begrense omfanget*. In *Rapport/Report 34/2015 NOFIMA*.

Moss, M. L. (1961). Studies of the acellular bone of teleost fish. I. Morphological and systematic variations. *Acta Anatomica*, *46*, 343–462. https://doi.org/10.1159/000141794

Moss, M. L. (1962). Studies of the acellular bone of teleost fish. II. Response to fracture under normal and acalcemic conditions. *Acta Anatomica*, *48*, 46–60. https://doi.org/10.1159/000141826

Moss, M. L. (1963). The biology of acellular teleost bone. *Annals New York Academy of Sciences*, *31*(109), 337–350. https://doi.org/10.1111/j.1749-6632.1963.tb13475

Nie, C.-H., Wan, S.-M., Tomljanovic, T., Treer, T., Hsiao, C.-D., Wang, W.-M., & Gao, Z.-X. (2017). Comparative proteomics analysis of teleost intermuscular bones and ribs provides insight into their development. *BMC Genomics*, *18*(1), 147. https://doi.org/10.1186/s12864-017-3530-z

Olsen, S. H., Siikavuopio, S. I., Tobiassen, T., Ageeva, T. N., & Heia, K. (2021). *Kvalitet på regnbueørret oppdrettet i sjø – holdbarhet (QIM), filetfarge og muskeltekstur. In Rapport/Report 7/2021*. NOFIMA.

Patterson, C., & Johnson, G. D. (1995). The intermuscular bones and ligaments of teleostean fishes. *Smithsonian Contributions to Zoology*, *559*, 1–83. https://doi.org/10.5479/si.00810282.559

Roberts, R. J. (2012). *Fish pathology* (4th ed.). Wiley-Blackwell.

Roberts, R. J., Hardy, R. W., & Sugiura, S. H. (2001). Screamer disease in Atlantic salmon, *Salmo salar* L., in Chile. *Journal of Fish Diseases*, *24*(9), 543–549. https://doi.org/10.1046/j.1365-2761.2001.00328.x

Rosa, J. T., Laizé, V., Gavaia, P. J., & Cancela, M. L. (2021). Fish models of induced osteoporosis. *Frontiers in Cell and Developmental Biology*, *9*, 672424. https://doi.org/10.3389/fcell.2021.672424

Schindeler, A., McDonald, M. M., Bokko, P., & Little, D. G. (2008). Bone remodeling during fracture repair: The cellular picture. *Seminars in Cell and Developmental Biology*, *19*(5), 459–466. https://doi.org/10.1016/j.semcdb.2008.07.004

Smith-Vaniz, W. F., Kaufman, L. S., & Glowacki, J. (1995). Species-specific patterns of hyperostosis in marine teleost fishes. *Marine Biology*, *121*, 573–580. https://doi.org/10.1007/BF00349291

Soliman, S. A. (2018). The growth cartilage and beyond: Absence of medullary bone in silver carp ribs. *Mathews Journal of Cytology and Histology*, *2*(1), 8.

Takeyama, K., Chatani, M., Takano, Y., & Kudo, A. (2014). In-vivo imaging of the fracture healing in medaka revealed two types of osteoclasts before and after the callus formation by osteoblasts. *Developmental Biology*, *394*(2), 292–304. https://doi.org/10.1016/j.ydbio.2014.08.007

Trangerud, C., Bjørgen, H., Koppang, E. O., Grøntvedt, R. N., Skogmo, H. K., Ottesen, N., & Kvellestad, A. (2020). Vertebral column deformity with curved cross-stitch vertebrae in Norwegian seawater-farmed Atlantic salmon, *Salmo salar* L. *Journal of Fish Diseases*, *43*(3), 379–389. https://doi.org/10.1111/jfd.13136

Usher, M. L., Talbot, C., & Eddy, F. B. (1988). Drinking in Atlantic Salmon Smolts transferred to seawater and the relationship between drinking and feeding. *Aquaculture*, *73*(1), 237–246. https://doi.org/10.1016/0044-8486(88)90058-0

Weigele, J., & Franz-Odendaal, T. A. (2016). Functional bone histology of zebrafish reveals two types of endochondral ossification, different types of osteoblast clusters and a new bone type. *Journal of Anatomy*, *229*(1), 92–103. https://doi.org/10.1111/joa.12480

Weiss, R. E., & Watabe, N. (1979). Studies on the biology of fish bone. III. Ultrastructure of osteogenesis and resorption in osteocytic (cellular) and anosteocytic (acellular) bones. *Calcified Tissue International*, *28*(1), 43–56. https://doi.org/10.1007/BF02441217

Willett, C. E., Cortes, A., Zuasti, A., & Zapata, A. G. (1999). Early hematopoiesis and developing lymphoid organs in the zebrafish. *Developmental Dynamics*, *214*(4), 323–336. https://doi.org/10.1002/(SICI)1097-0177(199904)214:4<323::AID-AJA5>3.0.CO

Witten, P. E., Gil-Martens, L., Huysseune, A., Takle, H., & Hjelde, K. (2009). Towards a classification and an understanding of developmental relationships of vertebral body malformations in Atlantic salmon (*Salmo salar* L.). *Aquaculture*, *295*(1), 6–14. https://doi.org/10.1016/j.aquaculture.2009.06.037

Witten, P. E., & Hall, B. K. (2002). Differentiation and growth of kype skeletal tissues in anadromous male Atlantic Salmon (*Salmo salar*). *International Journal of Developmental Biology*, *46*, 719–730.

Witten, P. E., Hansen, A., & Hall, B. K. (2001). Features of mono- and multinucleated bone resorbing cells of the zebrafish *Danio rerio* and their contribution to skeletal development, remodeling, and growth. *Journal of Morphology*, *250*(3), 197–207. https://doi.org/10.1002/jmor.1065

Witten, P. E., & Huysseune, A. (2009). A comparative view on mechanisms and functions of skeletal remodelling in teleost fish, with special emphasis on osteoclasts and their function. *Biological Reviews Cambridge Philosophical Society*, *84*(2), 315–346. https://doi.org/10.1111/j.1469-185X.2009.00077.x

Witten, P. E., Villwock, W., Peters, N., & Hall, B. K. (2000). Bone resorption and bone remodelling in juvenile carp, *Cyprinus carpio* L. *Journal of Applied Ichthyology*, *16*(6), 254–261. https://doi.org/10.1046/j.1439-0426.2000.00233.x

Yao, J., & Mørkøre, T. (2017). *Mechanical properties of the vertebral column and ribs of farmed fish with emphasis on Atlantic Salmon*. Mater Thesis, Norwegian University of Life Sciences, Ås.

How to cite this article: Brimsholm, M., Fjelldal, P. G., Hansen, T., Trangerud, C., Knutsen, G. M., Asserson, C. F., Koppang, E. O., & Bjørgen, H. (2023). Anatomical and pathological characteristics of ribs in the Atlantic salmon (*Salmo salar* L.) and its relevance to soft tissue changes. *Anatomia, Histologia, Embryologia*, *52*, 421–436. https://doi.org/10.1111/ahe.12900